

## Contents lists available at ScienceDirect

## MethodsX

journal homepage: www.elsevier.com/locate/mex



# ModMag: A modular magnetic micro-robotic manipulation device



Max Sokolich, David Rivas, Yanda Yang, Markos Duey, Sambeeta Das\*

Department of Mechanical Engineering, University of Delaware, 130 Academy St, Newark, 19717 DE, United States of America

#### ARTICLE INFO

#### Method name: Modular Magnetic Manipulation Device

Keywords:
Micro-robotics
Cellular manipulation
Magnetic actuation
Electromagnets
Magnetic tweezers

#### ABSTRACT

Electromagnetic systems have been used extensively for the control of magnetically actuated objects, such as in microrheology and micro-robotics research. Therefore, optimizing the design of such systems is highly desirable. Some of the features that are lacking in most cur- rent designs are compactness, portability, and versatility. Portability is especially relevant for biomedical applications in which in vivo or in vitro testing may be conducted in locations away from the laboratory microscope. This document describes the design, fabrication, and imple- mentation of a compact, low-cost, versatile, and user-friendly device (the ModMag) capable of controlling multiple electromagnetic setups, includ- ing a two-dimensional 4-coil configuration, a 3-dimensional Helmholtz configuration, a 2-dimensional magnetic tweezer configuration, and a piezoelectric transducer for producing acoustic waves. All electronics for powering the systems are contained in a compact  $10^{\prime\prime}$ x6"x3" case, which includes a  $10^{\prime\prime}$  touchscreen. A graphical user interface provides additional ease of use. The system can also be controlled remotely, allowing for more flexibility and the ability to interface with other software running on the remote computer such as proprietary camera software. Aside from the software and circuitry, we also describe the design of the electromagnetic coil setups and provide examples of the use of the ModMag in experiments.

- Low cost and portable magnetic micro-robot manipulation device
- Compatible with the 3 most common coil configurations (traditional, Helmholtz, tweezer)

## Table 1 Specifications table

Subject Area: More Specific Subject Area: Name of Your Method: Name and Reference of Original Method: Resource Availability: Mechanical Engineering: Micro-Robotics Magnetic Manipulation Systems Modular Magnetic Manipulation Device Not Applicable CAD Files and Software Available Upon Request.

#### Introduction

## Background

Electromagnets generate magnetic fields by moving current through a con- ductor. Systems that use electromagnets have important uses in a variety of applications. The systems and applications can range in size from several micrometers to several meters. A common example of a large-scale electromag- netic system is a scrap magnet. This system uses an enormous electromagnet capable of generating

E-mail addresses: sokolich@udel.edu (M. Sokolich), drivas@udel.edu (D. Rivas), robotyyd@udel.edu (Y. Yang), markosd@udel.edu (M. Duey), samdas@udel.edu (S. Das).

https://doi.org/10.1016/j.mex.2023.102171

Received 14 November 2022; Accepted 3 April 2023

Available online 3 April 2023

2215-0161/© 2023 The Author(s). Published by Elsevier B.V. This is an open access article under the CC BY-NC-ND license (http://creativecommons.org/licenses/by-nc-nd/4.0/)

<sup>\*</sup> Corresponding author.

strong magnetic fields for sorting out and transporting metal scraps [1]. On the other end of the spectrum, an electron beam physical vapor deposition chamber is a device that vaporizes a target material and uses this to coat a very thin and consistent layer of the material onto a substrate. In order to create sufficient power to vaporize the target material, a strong magnetic field is generated by an electromagnet and used to focus and con- centrate the electrons from the power source [2]. Other applications include MRI, magnetic particle imaging, microrheology, active matter systems, and micro-robotics.

Electromagnetic actuation also has the ability to actuate magnetic objects untethered, i.e. without touching them. This is particularly useful in micro-robotics in which the small size of the micro-robots makes tethered actuation impractical.

Micro-robots have drawn a lot of attention in recent years due to their potential to radically improve the efficacy of numerous tasks, such as cell manipulation, targeted drug delivery, microsurgery, and mixing of particles [3]. Despite this, conventional methods for powering macro-scale robotic actuation methods do not apply at the micro-scale, since they cannot be scaled down sufficiently. Hence, autonomous and reliable control of these micro-robots is an on going challenge. Different methodologies have been proposed in recent years in a bid to efficiently control micro robots. Researchers have demonstrated the actuation of micro machines by employing bubble creation using chemical reactions [4] or by attaching the synthetic micro-robots to swimming bacteria [5]. External magnetic, acoustic, or electric fields have also been employed to control and steer the micro-robots [5–7].

One of the most common methods of controlling micro-robots is magnetic actuation. Magnetic actuation has multiple advantages over other actuation methods; One example, is their untethered actuation capability, making it possible to deploy the micro-robots in a variety of environments. In addition, magnetic fields are regarded as a safe choice to use at the cellular and tissue level for a large number of biomedical applications, and can generate relatively large forces [8].

Examples of previous electromagnetic actuation mechanisms for micro- robotic control are now described. Ryan et al. created a magnetic actuation system using permanent magnets attached to stepper motors. The stepper motors spun to create a rotating magnetic field, which resulted in the rolling of a magnetic micro-robot [9]. Yuan et al. developed Rectmag3D, which used rectangular coils to achieve 5 degrees of freedom (DoF) control of a milli/micro- robot in 3D working space [10]. OctoMag is an electromagnetic system capable of 5 DoF manipulation that uses large, complicated, and expensive equipment [11]. Floyd et al. created a magnetic system capable of actuating a  $250 \times 130 \times 100$  um micro-robot using 6 electromagnetic coils [12]. Zhang et al. developed a 3D magnetic tweezer system capable of translating magnetic microbeads using high gradient magnetic fields [13]. Yang et al. used an array of 4 traditional electromagnetic solenoid coils and 1 ring coil to actuate a magnetic fungus spore using rotating magnetic fields. There has also been research into the opti- mization and design of a 2D magnetic gradient-based micro-robotic actuation system for in vitro and in vivo applications [14]. Yu et al. constructed a spe- cialized coil system consisting of both Helmholtz and Maxwell coils, capable of both consecutive locomotion and drilling of a magnetic micro-robot [15].

The examples listed above all use expensive equipment such as data acqui- sitions devices and large bench top power supplies which limit their ability to be used on other microscopes or transported to other locations. Further- more, the software is generally integrated onto a lab computer which also limits portability. In determining the design of the portable electromagnetic system we focused on three aspects. The first was that the software and cir- cuitry should be versatile in its ability to be used with multiple electromagnetic setups and, therefore, micro-robots with different actuation mechanisms. That is, it is desirable for a system to be versatile and not require a complete system redesign when using different micro-robots or during different applications or experiments. The electromagnetic setups we focused on were a 2D solenoid array, a 3D Helmholtz-based, and a 2D magnetic tweezer system. Each of these systems allows for immense versatility when it comes to micro-robotic experi- ments. We also sought to create a portable and inexpensive system that could also be used easily. Making the system portable and using a standalone design allows for the system to be transferable to different microscopes and imaging systems and also to settings outside the lab which could be useful in medical applications. We also expanded its control capabilities to include acoustic actuation, therefore allowing both acoustic driven and electromagnetic driven microrobotic motility control. We demonstrate this unique ability by switch- ing seamlessly between magnetic rolling and acoustic actuation of a single microrobot.

As described above, three designs were used: a traditional 2D coil system, a 3D Helmholtz-based coil system, and a 2D magnetic tweezer system, all of which can be used simultaneously with acoustic actuation via a transducer. The designs of each are discussed in the following sections. In this paper, we demonstrate the design and testing of a handheld, portable, low cost, modular electromagnetic actuation device, ModMag, for control of micro-robots. We also show experimental examples of micro-robot control using different types of magnetically driven micro-robots for applications in extracellular research.

## ${\it Electromagnetism}$

When an electric current passes through a wire, the movement of charge generates a magnetic field. A solenoid, or electromagnet, uses many of these wires wrapped concentrically around a cylinder to create a magnetic field in a direction along its central axis. The strength of the magnetic field is pro- portional to the current and increases with the number of times the wire is wrapped around the cylinder. It is also proportional to the magnetic perme- ability which can be increased by introducing materials with high magnetic permeability into the core of the solenoid. Generally, ferromagnetic materials with low coercivity, such as soft iron, are the material of choice for their abil- ity to enhance the magnetic field generated by the solenoid while retaining low magnetization when the current is turned off.

Ferromagnetic materials contain microscopic magnetic domains where groups of magnetic moments naturally align in the same direction. When the domains are all aligned randomly the material is demagnetized. However, the presence of an external magnetic field can align the domains in the direction of the applied field, causing the material to be magnetized. It may be helpful to think of

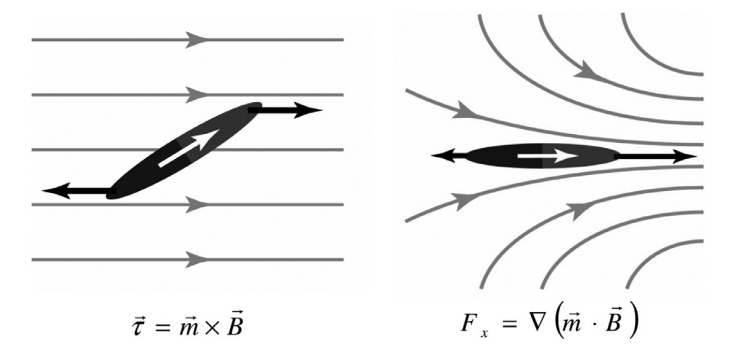


**Fig. 1.** The left figure shows an object rotating due to a magnetic torque. The white arrow indicates the object's magnetic moment and the gray lines represent magnetic field lines. The figure on the right shows an object moving due to a magnetic force created by a magnetic field gradient [16]. The region to the right of the object has a greater density of field lines which corresponds to a higher magnetic field strength.

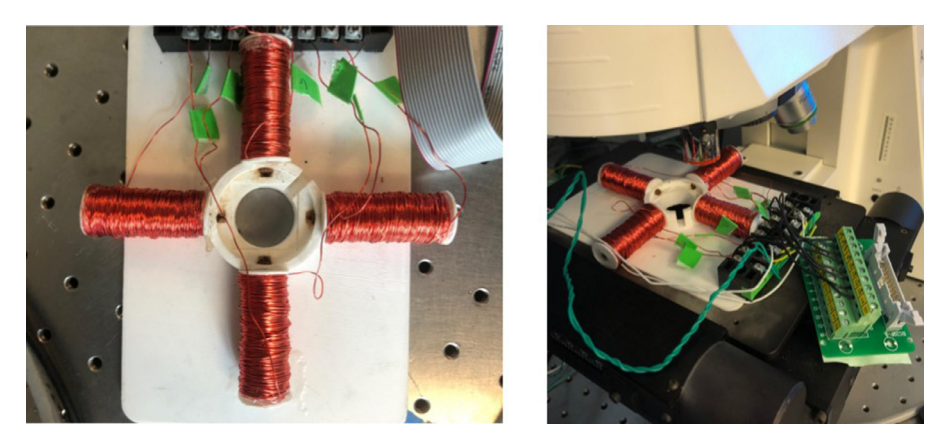


Fig. 2. 2D electromagnetic stand.

each of the magnetic domains as tiny magnets; when current passes through the surrounding coil of wire, it forces each of these tiny magnets in the same direction, thereby amplifying the field.

In a similar manner, when a ferromagnetic object, such as a magnetic micro-robot, is placed in a magnetic field, its magnetic moment aligns with the external field. This is the fundamental way in which magnetic micro-robots are controlled. One example of this is the magnetic steering of a self propelled, spherical, iron coated micro-sphere suspended in a liquid solution. Typically, the micro-sphere moves in an arbitrary direction and is subject to Brownian rotational fluctuations. An external torque can be applied in order to steer the microsphere in a particular direction. The torque,  $\Gamma$ , is given by

$$\Gamma = \mathbf{m} \times \mathbf{B} \tag{1}$$

where m is the magnetic moment of the micro-robot and B is the magnetic field. This torque therefore allows one to magnetically orient the micro-robots.

Magnetic forces can also be applied to the micro-robots by applying magnetic gradients. The magnetic force, F, is given by

$$\mathbf{F} = (\mathbf{m} \cdot \nabla)\mathbf{B} \tag{2}$$

Applying sufficiently strong magnetic gradients generally requires the use of high permeability poles which are used to concentrate the magnetic flux gener- ated from an electromagnetic. This allows for strong enough magnetic gradient forces to overcome the highly viscous drag forces that a micro-robot expe- riences. Magnetic devices that are used to magnetically manipulate objects are known as magnetic tweezers. Fig. 1 illustrates the process by which an object with a magnetic moment can be oriented or translated in a uniform or spatially varying field, respectively.

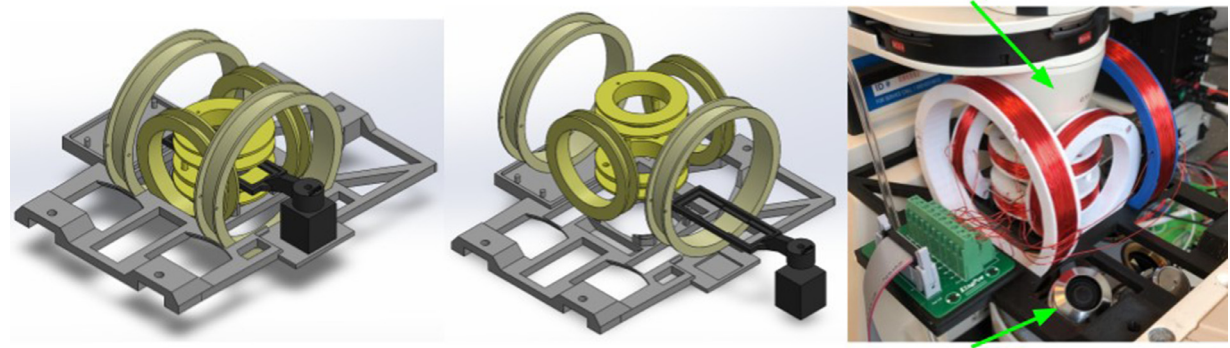
#### Method details

## Mechanical

## 2D Traditional coils

The traditional 2D electromagnetic setup consists of a 3D printed rectangular exchangeable stand that fits inside the microscope slide holder, and 4 perpendicular electromagnets (see Fig. 2). The stand was designed such that it fit onto the mechanical stage of a

# Condenser Lens



Objective Turret

Fig. 3. Design schematics and image of the 3D Helmholtz-based System.

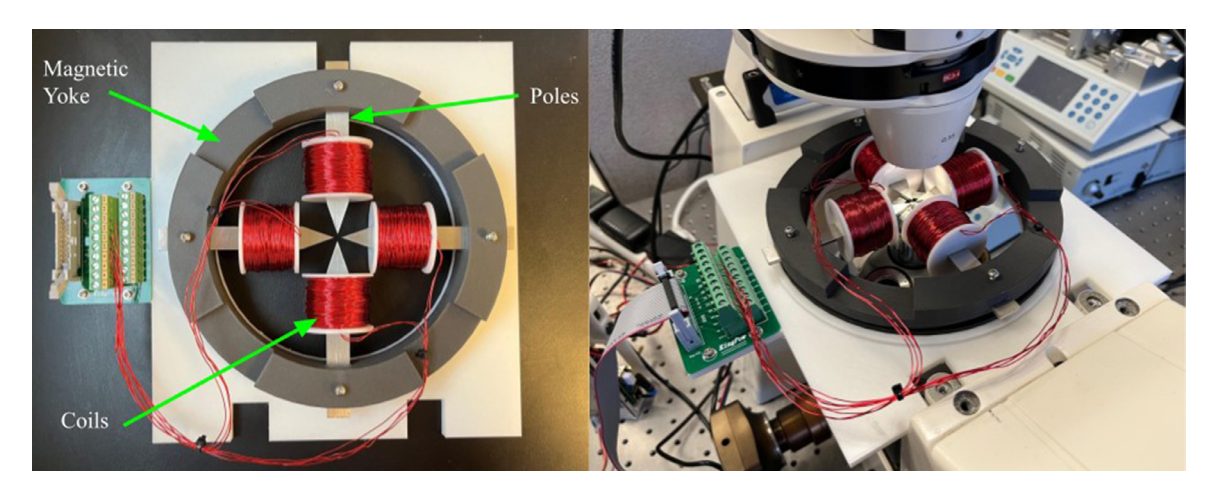


Fig. 4. Quadrupole Magnetic Tweezer System.

Zeiss Axioplan 2 upright microscope, however it can be placed on any microscope stage surface. The Axioplan 2's limited stage space of approximately  $150 \times 100 \times 25$  cm in volume made it difficult to design a stand with sufficient magnetic strength and negligible dis-ruption of the microscope's functionality. As a result both the stand and the electromagnetic coils were designed to be as compact as possible.

The 2D electromagnetic stand was designed in Solidworks and consists of only one part. The height of the stand measures roughly 23 mm to accommodate for the rotation of all microscope objectives in the objective turret. The region of interest was designed such that a standard  $22 \times 22$  mm cover-slip or  $25 \times 25$  mm square glass slide could be loaded with the desired samples roughly half way up the height of the stand. In addition, a 30 mm petri dish fits perfect in the region of interest. This allows for the electromagnets to point directly towards the samples. In addition, a custom square-shaped holder avoids the need to use a microscope slide which would require the electromagnets to rest at an angle. A slit in the stand was introduced to allow for easy insertion and removal of the cover slip using laboratory tweezers. The electromagnetic stand was printed on a Comgrow Creality Ender 3 Pro 3D printer using 1.75 mm, white PLA filament. An STL file of the stand was uploaded to Creality's Cura software with the following settings: printing temperature: 200 C, bed temperature 60 C, speed: 50 mm/s, layer height: 0.12 mm, and infill: 20. The rest of the settings were left as default. These settings provide a strong and durable stand for the electromagnets to rest upon. Four equally spaced holes 5 mm in diameter were created along the same plane as the cover slip holder allowing for the insertion of each electromagnet core. The holes allow for the electromagnetic core to be as close to the cover slip as possible.

The electromagnetic core material is AISI 1008 carbon steel made of 99.31- 99.7% iron, cold drawn and annealed at 925 °C. The cores had raw dimensions of 5 mm in diameter by 200 mm long. The relative permeability of the core was listed as  $(86 \pm 3.61)$  H/m. The cores were then cut to 50 mm long. 24 AWG magnet wire was used for the electromagnetic coils. In order to prevent the coil from unraveling, plastic end caps of 30 mm in diameter were cut from 0.7 mm in thickness plastic. 5 mm holes were then drilled into the center of these circles to allow for the electromagnetic core to be inserted. To create an electromagnet, one end cap is positioned at the end of the core and glued in place using Gorilla 2 part epoxy. The second end cap is then glued 50 mm from the first end cap, or 5 mm from the opposite side. As a result, the electromagnetic coil will be 50 mm long, leaving 5 mm at one side to be inserted

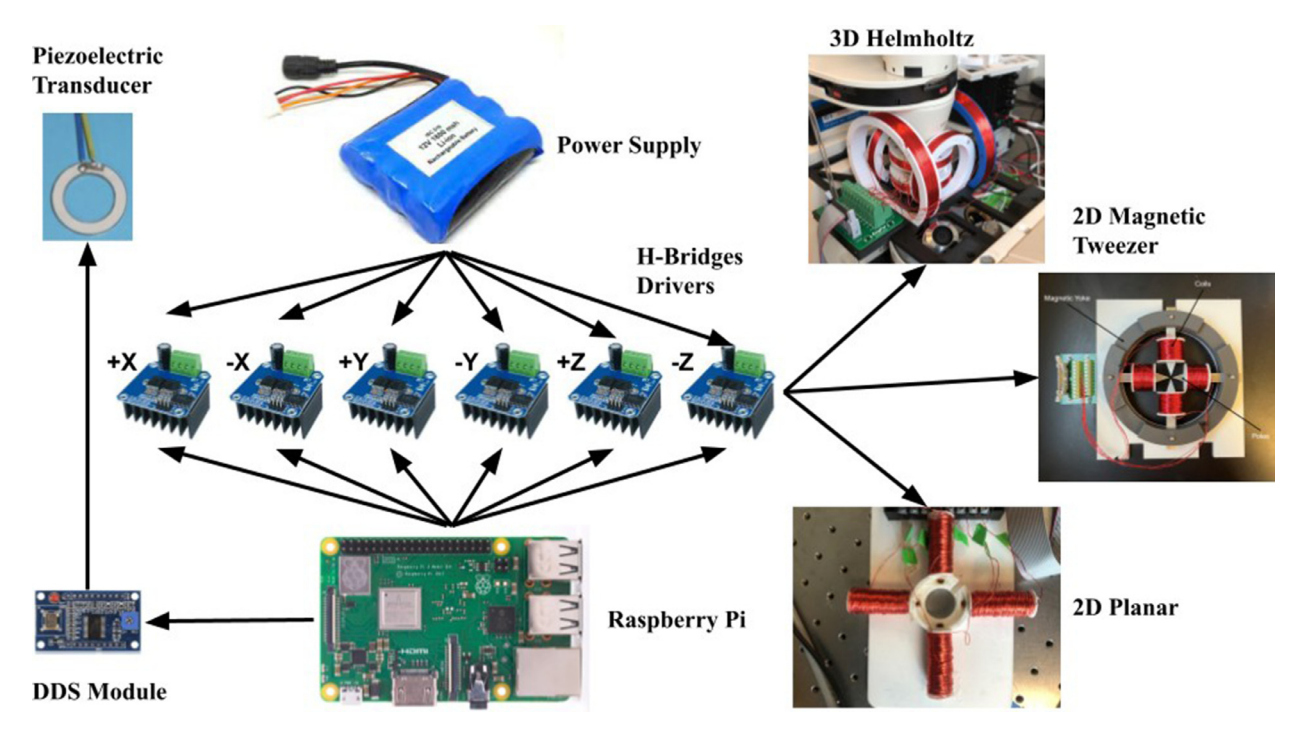


Fig. 5. Electrical Schematic.

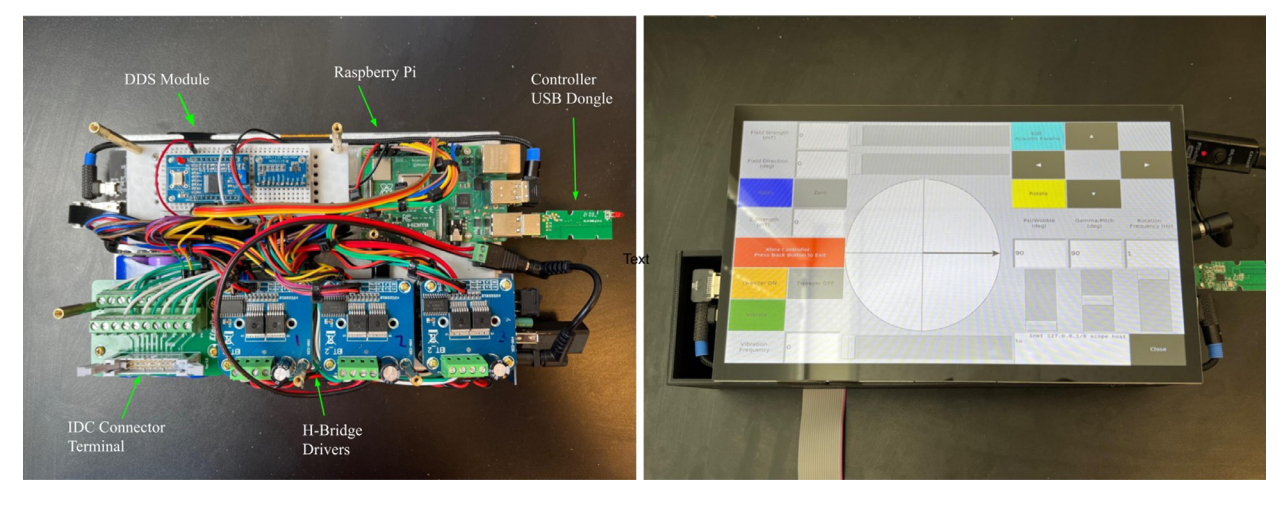


Fig. 6. Electrical circuitry mounted to the back of the display touchscreen. Not pictured is a 3D printed case to house the electronics.

into the stand. Coils were then wound carefully using an electric drill to exactly 980 turns of the 24 AWG magnet wire. Using a Tesla meter, the electromagnetic strength at the face of the coil was measured to be  $(201 \pm 3)$  mT at a current of 2 Amps, and around 15 mT at the center of the work space. The six electromagnet's were then inserted and glued into the six holes in the 3D printed stand.

#### 3D Helmholtz-Based system

A 3D electromagnetic manipulation system was designed for micro-robotic applications involving rotating homogeneous magnetic fields, which is well suited for 3D magnetic steering or magnetic rolling. The custom coil system is inspired by a Helmholtz design and is designed for mounting on the Zeiss Axiovert 200 M inverted microscope (see Fig. 3). Measurements of the micro-scope bed dimensions and distances between lenses were recorded. These size constraints then defined the maximum radii for the coil rings. Calipers were used to determine the microscope measurements. The Helmholtz coil system consists of three pairs of rings each sharing their respective common axis. The rings are wrapped with copper wire to form coils. As mentioned above, to attain an optimally uniform field the distance between pairs of rings should be equal to their radius. However, this is difficult to achieve in practice and is also generally unnecessary for micro-robotic applications, therefore we loos- ened this constraint in order to allow the system

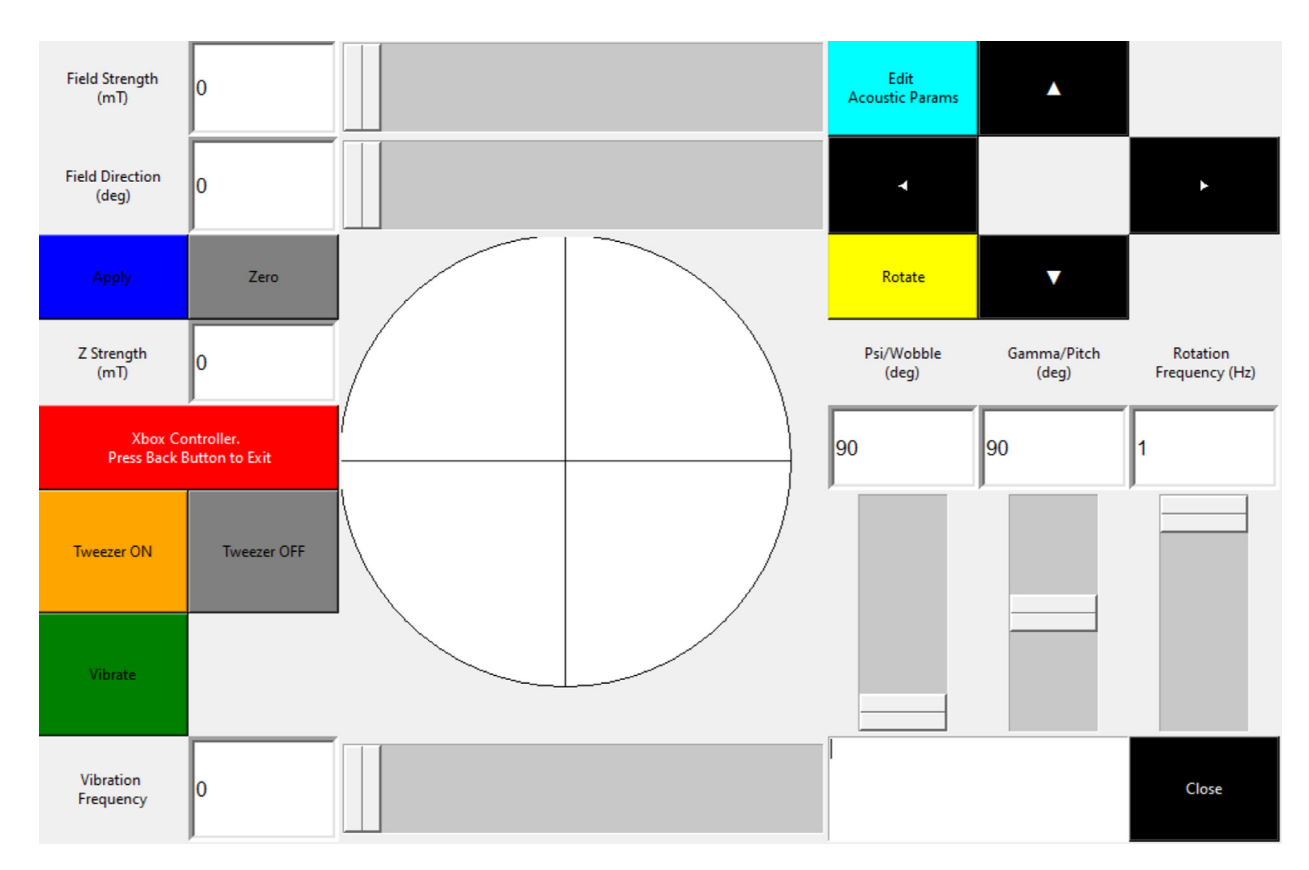


Fig. 7. GUI python control panel displayed on 10 inch touchscreen. All circuitry mounted on backside of device.

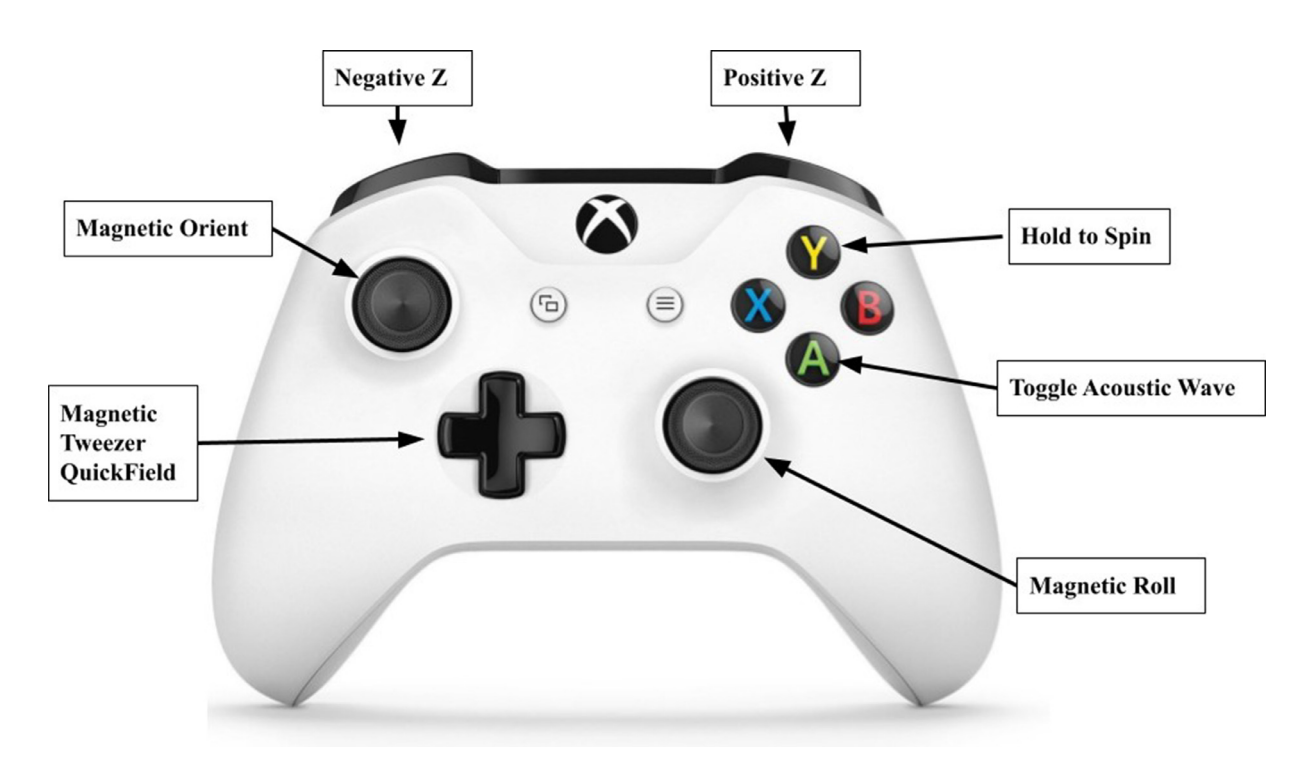
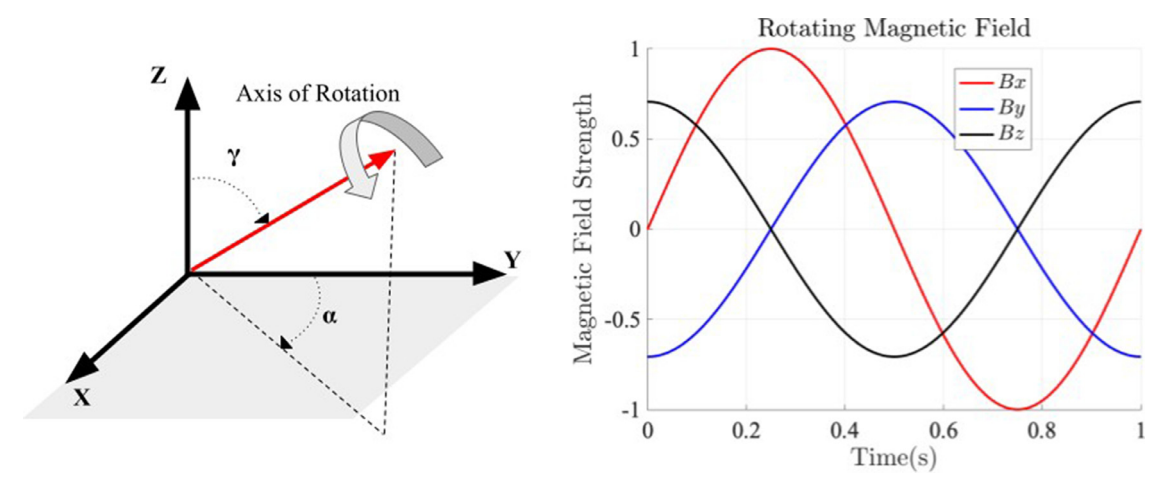


Fig. 8. Gaming controller button layout with respective Micro-robotic operations.



**Fig. 9.** Left: Schematic illustrating the effect of  $\alpha$  and  $\gamma$  on rotation axis of micro-robot. Right: A 1 Hz rotating magnetic field plotted using Eqs. (3),(4), and (5). 1 Hz sine waves with  $\gamma = 45^{\circ}$  and  $\alpha = 90^{\circ}$  over a 1 second interval.

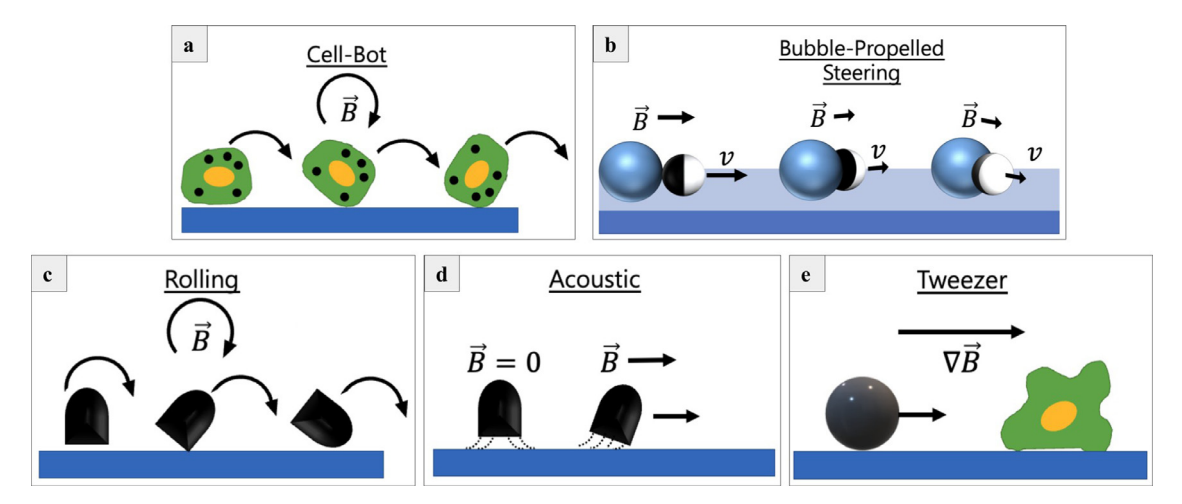
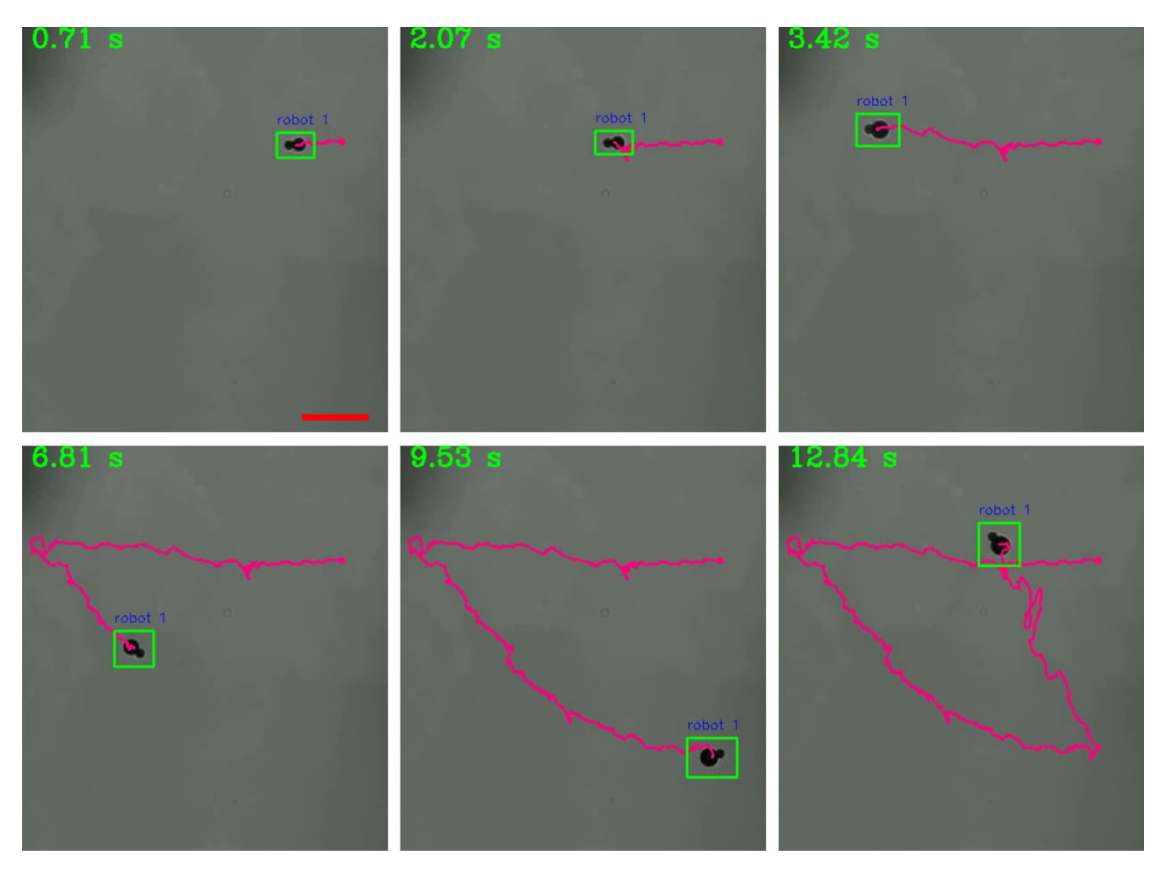


Fig. 10. The 5 micro-robotic actuation mechanisms that can be achieved using the ModMag device.

to better fit the workspace. As we will discuss later, we find that this system performs very well for magnetic steering and rolling applications for which it was designed.

To optimally fit in the workspace, the large and medium sized rings were mounted on the stage vertically while the small rings were mounted horizon- tally, as shown in Fig. 3. Microscope dimensions allow for a maximum diameter of 106 mm for the large rings without interfering with the objective turret, and a minimum diameter of 36 mm for the small rings without interfering with the condenser lens. The smallest pair of rings are spaced such that their distance,  $H_s$ , is equal to their radius,  $H_s = R_s = 26$  mm (both measured center-to- center). The medium sized pair has a radius of  $R_m = 35$  mm and is spaced slightly farther apart ( $H_m = 66$  mm). For the largest pair of rings,  $R_l = 54$  mm and  $H_l = 84$  mm. As a result, the ratios of distance over radius of the small, medium, and large pairs of rings are 1, 1.9, and 1.6, respectively. The platform unit is roughly 230 mm long and 140 mm wide with integrated slots for mount- ing on the microscope. On either side of the platform is an area for mounting a motherboard with electrical connections, and a square divot for mounting a 2-axis micrometer for slide arm micro-translation. The slide arm fits both a conventional glass microscope slide as well as square cover-slips. Four slots are outfitted within the platform to hold the large and medium coils with a tran- sition fit. The small coil pair sits on four stilts, while four small pegs separate the coil pair.

The platform, slide arm, and rings were designed within Solidworks CAD software and printed using 3D Printing methods. All components are printed with PLA using an Ender 3 Pro. Structural properties of PLA allow for ade- quate rigidity within the frame to hold the weight of the primary components. The coils are wrapped with 24 AWG copper wire using a standard hand drill to achieve more uniform wire layers than what is achieved by hand. In order to connect the ring to the drill, a drill adapter unit consisting of three extending limbs was fabricated. Small pegs on each limb allowed for a transition fit into receiving holes on the rings. The resulting number of turns is approximately 368 for the small and medium coils and 260 for the large coils. Applying 1 A to each of the coils yields a uniform magnetic field over the sample area of 4 mT, 2 mT and 2 mT for the small, medium and large rings respectively. This allows for magnetic steering and rolling actuations of magnetic micro-robots, as shown in the experimental validation section.



**Fig. 11.** Trajectory of self bubble propelled magnetic microrobot on the air-water interface over approximately 13 s (see Video 1). The microrobot is a 25 um polystyrene micro- spheres coated in 100 nm Ni and 25 nm Pt. The fluctuations from a perfectly linear trajectory are due to subtle air currents moving the robot around. Scale-bar: 200 um.

#### 2D Magnetic tweezers

The 2D magnetic tweezers system for control of magnetic micro-robots utilizes a quadrople design and illustrated in Fig. 4. Its main components are divided into three parts, namely the yoke, poles, and coils. The yoke was designed using SolidWorks and subsequently fabricated using Protopasta Magnetic Iron Filled PLA through 3D printing. The yoke possesses an outer diameter of 180 mm and an inner diameter of 160 mm. The use of magnetic PLA provides several advantages, including completing the magnetic circuit to increase the efficiency of magnetic field generation, introducing high magnetic permeability to reinforce the magnetic field, and reducing the current required to decrease the heat generated by the coils.

Four magnetic poles are integrated into the yoke, with sharp tips oriented toward the center. Each pole is positioned on the same level and spaced  $90^{\circ}$  apart from one another. The distance between opposite tips is 3 mm. These poles are made using 1.5 mm Nickel-Iron soft ferromagnetic alloy (Mu- Metal, Magnetic Shield Corporation), a high-permeability material fabricated using laser cutting. This material allows efficient transport of magnetic flux from the coils to the tip.

Each magnetic pole has an electromagnetic coil fixed to it, comprising 600 turns of 24 AWG enameled Copper wire. The tip of the magnetic pole gener- ates a strong magnetic field gradient when the electromagnetic coil receives an input current, which then generates a magnetic force acting on the micro-robot. The measured magnetic field directly in front of a single pole was measured to be 120 mT at 2 A. Approximately 3 mm away from this pole, the field was measured to be approximately 40 mT. This results in a magnetic gradient of roughly 26 T/m. By applying different currents to different coils, the magnitude and direction of the micro-robot's motion can be changed based on the principle of force superposition.

The space availability constraint imposed by the microscope itself was a significant design consideration for this system. Consequently, the design may be modified depending on specific space constraints.

#### Electronics

## Components

The design of the electrical system is a key component of the versatile electromagnetic control system described in this document. This electrical system has been designed to work seamlessly with any of the electromagnetic setups discussed above. It is also being capable of standalone operation without being tethered to a single lab computer, providing portability. Portability was a top priority of the design and the system can be easily transported without the need for a bench-top external power supply. Computational

capability is pro- vided by a Raspberry Pi Model 3 B+, a small yet powerful computer that can run a complete operating system. To facilitate user interaction, a custom graphical user interface has been developed in Python and is displayed on a HMTECH 10.1 Inch Touchscreen Monitor with a resolution of  $1024 \times 600$ .

The computer is also equipped with 40 GPIO (general purpose input/out- put) pins, which can be controlled through software. However, as electromag- nets require high currents that cannot be powered directly from the GPIO pins, six SEEU. AGAIN BTS7960B 43A Double DC Stepper H-Bridge PWM drivers are employed to vary the current and polarity from an external power supply. These H-Bridges convert the user-defined currents generated from the GPIO pins and scale them accordingly to each electromagnet.

The external power supply comprises three Lithium-ion 18,650 batteries, providing 12 V with a peak current draw of 3 A. To facilitate charging, a charging circuit board with a DC barrel jack has been incorporated, allowing the batteries to be recharged when depleted. External power sources may also be used if desired. Connection between the controller and each of the three coil setups is facilitated through a 20-pin IDC cable with an associated female adapter terminal. The electrical schematic is presented in Fig. 5.

The ModMag system also includes a HiLetgo DDS AD9850 Signal Gen- erator Module, which is used to produce the signals required for actuating acoustic micro-robots. To achieve this, the signal generator chip is connected to a piezoelectric transducer that is mounted on a microscope slide. When acti- vated, the signal generator produces an electrical sine wave that is converted into pressure waves at the same frequency by the transducer. These pressure waves travel through the liquid medium on the slide's surface until they reach the acoustic micro-robot. Once there, they vibrate a small air bubble that is trapped inside a cavity, as described in [17] and [6]. This vibration generates an acoustic streaming force that propels the micro-robot forward. Typically, the signal generator module is a large bench-top device, given the high actuation frequencies involved (1–3 MHz). However, the ModMag controller and software integrate all the necessary features for actuating acoustic micro-robots into a single chip on the device, making it highly compact and portable.

#### Software

#### Description

To achieve precise real-time control of the current to each electromagnetic coil, a custom graphical user interface was developed in Python using the Tkinter and Gpiozero libraries Fig. 7. This intuitive software allows for the application of constant magnetic fields in any user-defined direction, as well as rolling, spin- ning, or vibrating functionalities. Additionally, the system can be controlled using a game controller to achieve even greater responsiveness and precision. To apply current and therefore produce a magnetic field, the user simply inputs the desired magnetic field direction and strength, which is then used to modulate the current sent to each coil. This involves breaking down the associated vector into its x and y components, and scaling the current sent through each coil proportionally to the magnetic field strength. Furthermore, to improve the field strength and uniformity, an opposite polarity signal is sent to the opposite-facing coil. For example, when a positive current is applied to the -x electromagnet coil, a simultaneous negative current will be applied to the +x coil, enhancing the magnetic field strength and uniformity.

The ModMag system includes a magnetic tweezer mode that allows the user to switch between "tweezer on" and "tweezer off" modes depending on the type of electromagnetic system being used. Magnetic tweezers utilize traditional coils to concentrate magnetic flux towards the poles, creating sufficient magnetic gradients to move a magnetic micro-robot without additional propulsion mechanisms. To optimize micro-robot movement, the magnetic moment should align with the magnetic gradient. Thus, when magnetic tweezer mode is enabled in the software, current is only sent through one pair of coils in order to align the magnetic moment with the field gradient. Note that the polarity of the magnetic field does not matter in this case since a single pole always acts to attract the micro-robots. This is because changing the polarity changes the sign of **B** and this also causes the micro-robot to rotate such that **m** aligns with B, hence changing the sign of **m** as well.

In addition to being controlled via the graphical user interface, all functions can be operated using a gaming controller, as illustrated in Fig. 8. When a button is pressed on the interface, it wirelessly connects to a USB gaming controller. The left joystick controls the orientation or tweezer functionalities in 360° while the right joystick adjusts the direction of a rolling magnetic microrobot, controlling the rotating magnetic field. The user can also generate a quick magnetic field gradient by using the 4 direction D-Pad on the controller. With the device, a rotating magnetic field can be generated in any user-defined direction, enabling precise and responsive control of a rolling micro-robot or an artificial bacteria flagella micro-robot/helical micro-robot. This is achieved by applying a time-varying sine wave to each of the X, Y, and Z axis coils, using the equations below:

$$B_{x} = A[\cos(\gamma)\cos(\alpha)\cos(\omega t) + \sin(\alpha)\sin(\omega t)] \tag{3}$$

$$B_{v} = -A[\cos(\gamma)\sin(\alpha)\cos(\omega t) + (\cos(\alpha)\sin(\omega t)] \tag{4}$$

$$B_{\tau} = A \sin(\gamma) \cos(\omega t) \tag{5}$$

Where  $\gamma$  is the azimuthal angle from the Z axis,  $\alpha$  is the polar angle from the X axis, A is magnetic field magnitude and  $\omega$  is the frequency which controls the speed of the rolling micro-robot. The default azimuthal angle for control- ling magnetic rolling micro-robots is 90°, whereas changing the polar angle allows the user to steer the micro-robot's direction Fig. 9. In contrast, changing both the azimuthal and polar angles provides full 3D maneuverability for helical micro-robot swimmers. The Y button feature allows the user to quickly switch between rolling and spinning actuation methods, which can also be achieved through the GUI by varying the value of gamma to 0° for clockwise spinning or 180° for counterclockwise spinning.

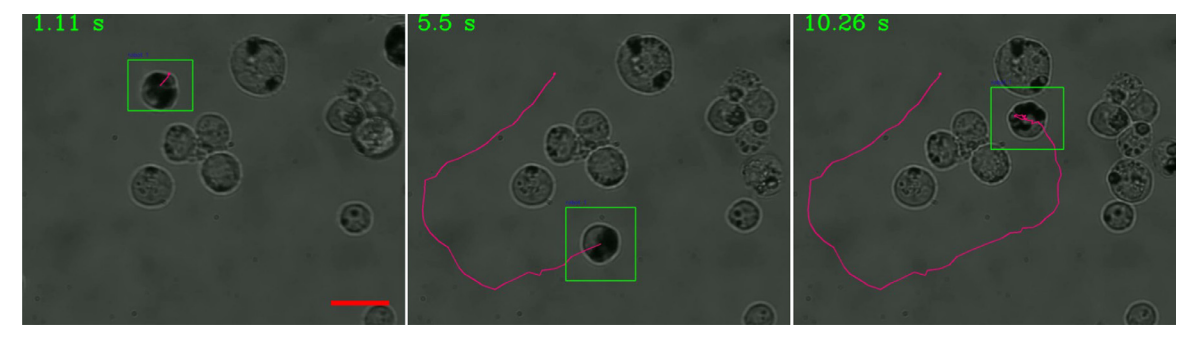


Fig. 12. Trajectory of a synthetically engineered Chinese hamster ovarian cell being manip- ulated by ingested magnetic microrobots (see Video 2). The micro-robots used were 4.8 um silica micro-beads coated with 100 nm of Nickel. Scale-bar = 20 um.

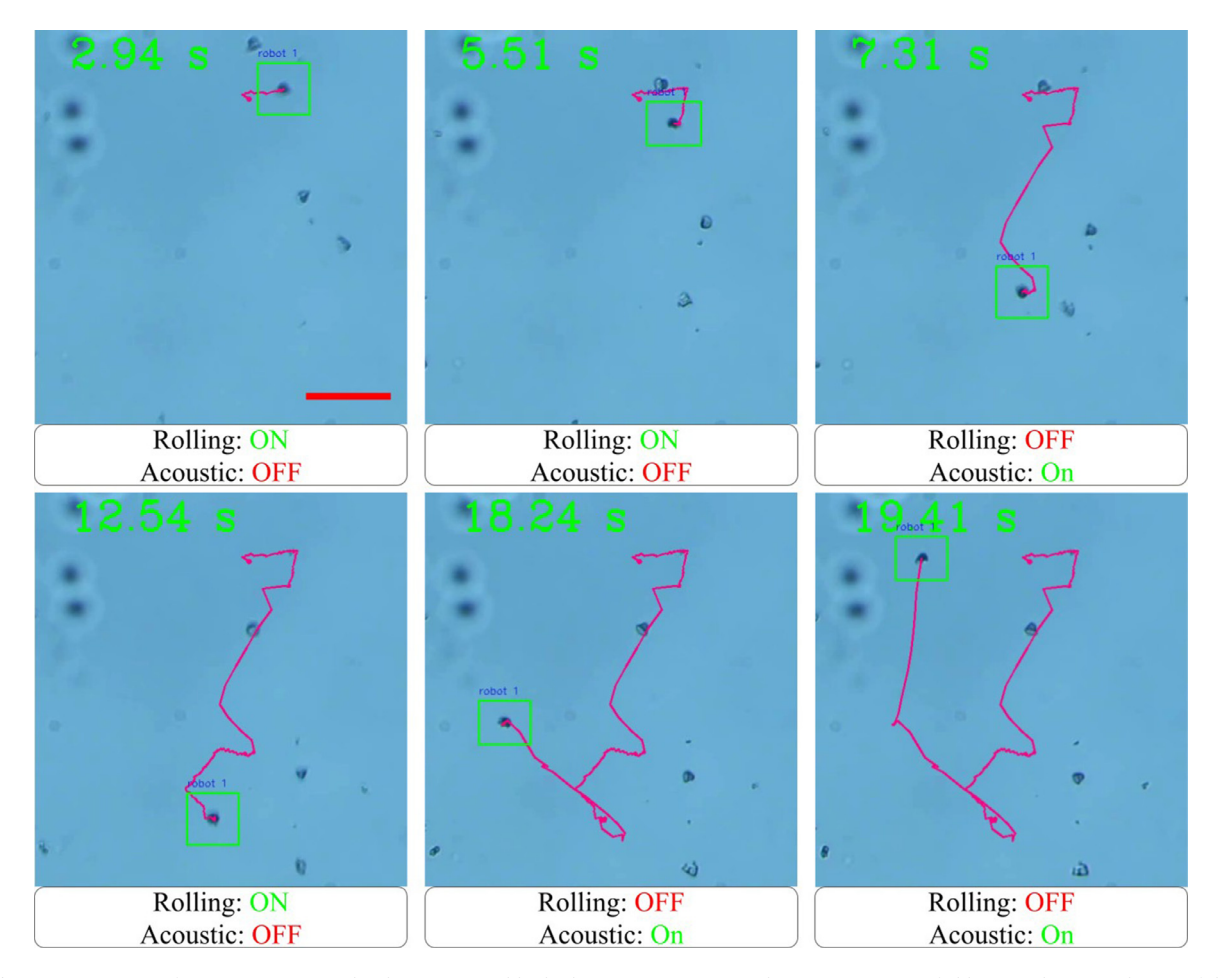


Fig. 13. Trajectory of an acoustic microrobot being actuated by both an acoustic wave and rotating magnetic field (see Video 3). Only one of the microrobots contained a trapped air- bubble and thus was able to be actuated via the acoustic waves. Scale-bar = 20 um.

In addition to the previously described functions, the graphical user inter- face offers additional options to control the microrobot. One such option is the ability to magnetically vibrate the micro-robot by turning on and off opposite facing electromagnets at user-defined frequencies. Moreover, there are quick direction buttons available that enable the user to apply magnetic fields in the  $\pm x$  or  $\pm y$  directions without having to use the slider to select specific angles.

Furthermore, the device employs a DDS signal generator module to control the frequency of a piezoelectric transducer and therefore actuate an acoust tic micro-robot. The user can adjust the frequency to actuate a range of acoustic micro-robots, and to turn on the module, the user can either use a button on the GUI or press the A button on the gaming controller. When the module is activated,

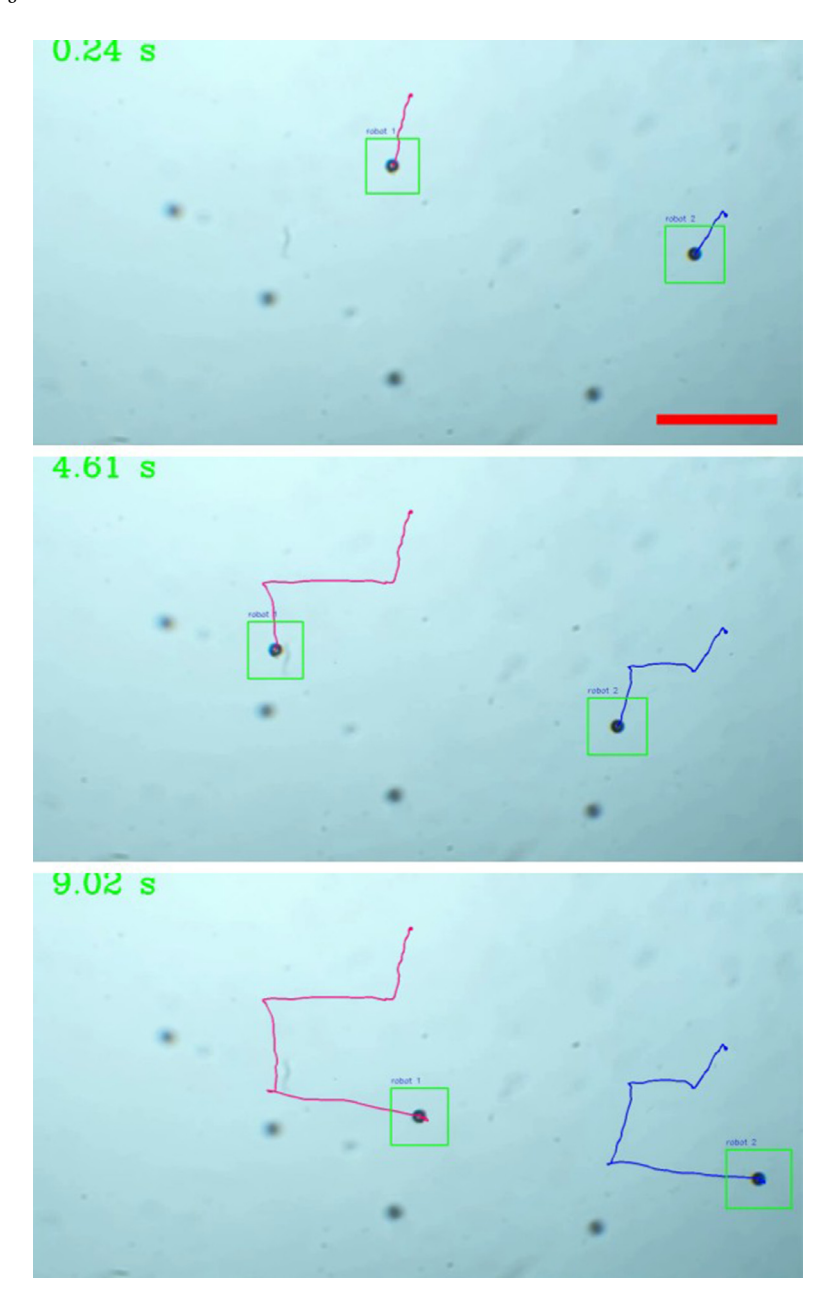


Fig. 14. Trajectories of two 25 um polystyrene microspheres coated with 100 nm Ni being actuated via the magnetic tweezers and ModMag device (see Video 4). Scalebar = 200 um.

the acoustic micro-robots self-propel, and the direction and orientation of the micro-robot can be adjusted using the magnetic field controller.

All of these functionalities can be controlled via the touchscreen display, or wirelessly via the PiGPIO daemon, which not only enables the GUI Python program to be run and controlled on any computer on the same Wi-Fi network but also allows for the integration of the magnetic control system with other software on the computer. For instance, the magnetic software can be used for real-time feedback control while tracking micro-robots using Python's OpenCV library and TrackPy.

## **Experimental validation**

As previously mentioned, the ModMag system boasts the capability to apply various signals to actuate a wide range of microrobotic actuation systems. Fig. 10 effectively illustrates these diverse actuation mechanisms. In the following paragraphs, we will proceed to experimentally validate each of these actuation mechanisms.

M. Sokolich, D. Rivas, Y. Yang et al. MethodsX 10 (2023) 102171

The 2D traditional coil setup has been employed to orient a variety of self-propelled micro-robots, such as electrophoretic or diffusiophoretic mag- netic Janus microspheres, or bubble-propelled micro-robots. To investigate the dynamics and control of platinum and nickel coated bubble-propelled micro-robots, Rivas et al. utilized the 2D system and controller described in [18]. Moreover, the researchers demonstrated the manipulation of passive polystyrene particles into the letters U and D for the University of Delaware, illustrating the versatility of the system. Fig. 11 displays the trajectory of a 25  $\mu$ m bubble-propelled micro-robot on the air-water interface, whose orientation or direction is regulated using the ModMag magnetic controller.

The 3D Helmholtz system is utilized to control various types of magnetic rolling micro-robots, such as micro-spheres coated with a hemisphere of nickel through electron beam deposition. In one instance, the 3D Helmholtz system was employed in [19] to showcase the ability to manipulate cells using rolling magnetic micro-robots. Moreover, the rotating magnetic field produced by the controller enables the rolling of Cell-bots, which are biological cells with magnetic micro-robots ingested inside. An illustration of this application is depicted in Fig. 12. The system has also been employed to actuate magnetic helical micro-robotic swimmers.

Fig. 13 showcases the combination of the DDS module and rotating magnetic field capabilities to steer acoustic micro-swimmers, which are created using the method described in [17]. The left joystick of the gaming controller is used to orient the micro swimmers while toggling the acoustic signal. The system also allows for rolling of the acoustic micro-swimmers with the acoustic signal on or off, providing more refined and flexible control options. This ability will be further studied in the future, potentially leading to enhanced individual robot and swarm control.

The magnetic tweezers system, as mentioned previously, utilizes high mag- netic field gradients to direct magnetic micro-beads and is applicable in cases where self-propulsion is not feasible or when high forces are required. An example of this system's capabilities is demonstrated in a study conducted by Mallick et al. [20], where the 2D magnetic tweezers system was employed to deliver paramagnetic micro-beads coated with Doxorubicin to cancer cells, leading to their death. Fig. 14 illustrates the trajectories of two 25 µm polystyrene microspheres coated in Nickel and moving through water on a microscope slide. The microspheres were actuated using the magnetic tweezers and the ModMag device.

#### Conclusion

In conclusion, we have successfully designed and constructed a compact, versatile, low-cost, and easy-to-use electromagnetic control system that can be paired with various electromagnetic systems, including traditional planar coils, 2D magnetic tweezers, and 3D Helmholtz-based coils. All of the systems can be used simultaneously with the integrated acoustic actuation using a piezo-electric transducer. The implementation of a graphical user interface has made the system user-friendly and easy to control. We plan to continue improving the system's versatility by upgrading the 2D magnetic tweezers to 3D and incorporating other micro-robotic off-board actuation methods, such as light actuation. With its portability, we believe that the system has the potential to be used in biomedical applications such as medical imaging systems for in vitro or in vivo experiments. Overall, we are excited about the future prospects of this system and its potential impact in advancing micro-robotic research.

### **Declaration of Competing Interest**

The authors declare that they have no known competing financial interests personal relationships that could have appeared to influence the work reported in this paper.

## **Data Availability**

Data will be made available on request.

## Acknowledgements

The authors gratefully acknowledge the late Richard West for his help with the cell lines. This project was supported by the Delaware INBRE pro- gram, with a grant from the National Institute of General Medical Sciences – NIGMS (P20 GM103446) from the National Institutes of Health and the State of Delaware. This work was also supported by NSF grant OIA2020973. This content is solely the responsibility of the authors and does not necessarily represent the official views of NIH.

#### Supplementary materials

Supplementary material associated with this article can be found, in the online version, at doi:10.1016/j.mex.2023.102171.

### References

- [1] HVR Magnetics. (2021, May 28). Common Questions About Scrap Magnet. HVR Magnetics Blog. https://www.hvrmagnet.com/blog/common-questions-about-scrap-magnet/ (Accessed on April 1, 2023)
- [2] Angstrom Engineering. (n.d.). Electron Beam Evaporation. Angstrom Engineering Tech Center. https://angstromengineering.com/tech/electron-beam-evaporation/ (Accessed on April 11, 2023)
- [3] K.E. Peyer, L. Zhang, B.J. Nelson, Bio-inspired magnetic swim- ming microrobots for biomedical applications, Nanoscale 5 (4) (2013) 1259–1272.
- [4] A.A. Solovev, Y. Mei, O.G. Schmidt, Catalytic microstrider at the air-liquid interface, Adv Mater 22 (39) (2010) 4340-4344.
- [5] M.S. Sakar, E.B. Steager, D.H. Kim, A. Agung Julius, M. Kim, V. Kumar, G.J. Pappas, Modeling, control and experimental characterization of microbiorobots, Int. J. Rob. Res. 30 (6) (2011) 647–658.

- [6] A. Aghakhani, O. Yasa, P. Wrede, M. Sitti, Acoustically pow- ered surface-slipping mobile microrobots, Proc Natl Acad Sci 117 (7) (2020) 3469-3477.
- [7] S. Das, E.B. Steager, M.A. Hsieh, K.J. Stebe, V. Kumar, Experiments and open-loop control of multiple catalytic microrobots, J. Micro- Bio Robot. 14 (1) (2018)
- [8] P. Fischer, A. Ghosh, Magnetically actuated propulsion at low reynolds numbers: towards nanoscale control, Nanoscale 3 (2) (2011) 557-563.
- [9] P. Ryan, E. Diller, Magnetic actuation for full dexterity micro-robotic control using rotating permanent magnets, IEEE Trans Rob 33 (6) (2017) 1398-1409.
- [10] S. Yuan, Y. Wan, S. Song, Rectmag3d: a magnetic actuation system for steering milli/microrobots based on rectangular electromagnetic coils, Applied Sci. 10 (8) (2020) 2677.
- [11] M.P. Kummer, J.J. Abbott, B.E. Kratochvil, R. Borer, A. Sengul, B.J. Nelson, Octomag: an electromagnetic system for 5-dof wireless micromanipulation, IEEE Trans Rob 26 (6) (2010) 1006–1017.
- [12] S. Floyd, C. Pawashe, M. Sitti, An untethered magnetically actuated micro-robot capable of motion on arbitrary surfaces, in: 2008 IEEE Inter-national Conference on Robotics and Automation, IEEE, 2008, pp. 419–424.
- [13] Zhang, X.: Magnetic gradient-based magnetic tweezer system for 3d and swarm control of microswimmer (2021)
- [14] D. Li, F. Niu, J. Li, X. Li, D. Sun, Gradient-enhanced electromagnetic actuation system with a new core shape design for microrobot manip- ulation, IEEE Trans Ind Electron 67 (6) (2019) 4700–4710.
- [15] C. Yu, J. Kim, H. Choi, J. Choi, S. Jeong, K. Cha, J.-o. Park, S. Park, Novel electromagnetic actuation system for three-dimensional locomotion and drilling of intravascular microrobot, Sens Actuators, A 161 (1–2) (2010) 297–304.
- [16] A.H.B.d. Vries,: High Force Magnetic Tweezers for Molecular Manipula- tion Inside Living Cells: proefschrift. s.n.], [S.1 (2004)
- [17] J.M. McNeill, N. Nama, J.M. Braxton, T.E. Mallouk, Wafer-scale fabri- cation of micro-to nanoscale bubble swimmers and their fast autonomous propulsion by ultrasound, ACS Nano 14 (6) (2020) 7520–7528.
- [18] D.P. Rivas, M. Sokolich, H. Muller, S. Das,: Dynamics and control of bubble-propelled microrobots. arXiv preprint arXiv:2203.13257 (2022)
- [19] D. Rivas, S. Mallick, M. Sokolich, S. Das,: Cellular Manipulation Using Rolling Microrobots, 6
- [20] S. Mallick, R. Abouomar, D. Rivas, M.S.S. Das,: Doxorubicin-Loaded Microbots for targeted drug delivery and anticancer therapy, 14